Electronic Supplementary Material (ESI) for Journal of Materials Chemistry A.
This journal is © The Royal Society of Chemistry 2017

Multicomponent (Mo, Ni) metal sulfide and selenide microspheres with empty nanovoids as anode materials for Na-ion batteries

Jin-Sung Park[a] and Yun Chan Kang[a,*]

[a]Department of Materials Science and Engineering, Korea University, Anam-Dong, Seongbuk-Gu, Seoul 136-713, Republic of Korea.

[*]Correspondence authors. E-mail: yckang@korea.ac.kr (Yun Chan Kang, Fax: (+82) 2-928-3584)

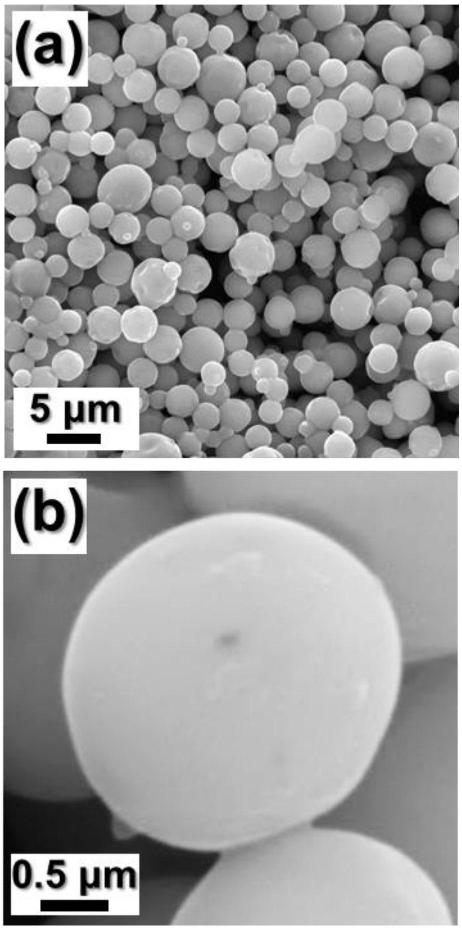

Fig. S1. Morphologies of the precursor microspheres obtained by spray drying process: (a) low resolution and (b) high resolution SEM images.

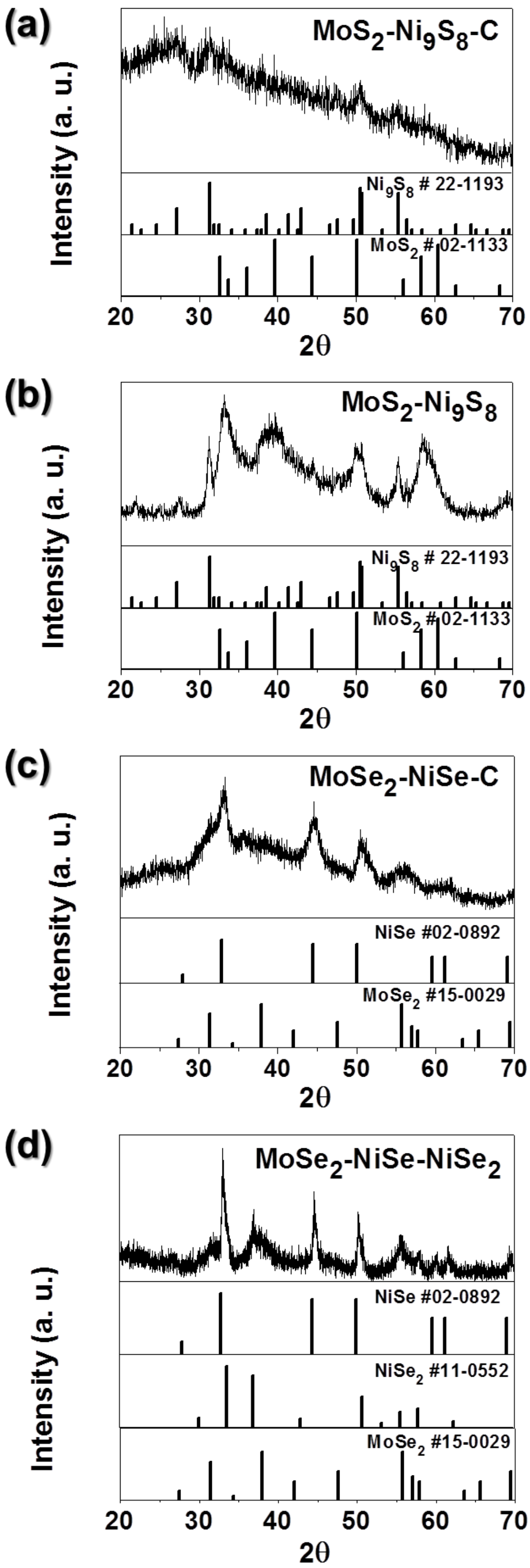

Fig. S2. XRD patterns of the multiroom-structured MoX_2-NiX_y (X= S or Se) and MoX_2-NiX_y-C microspheres. (a) MoS_2-Ni_9S_8-C, (b) MoS_2-Ni_9S_8, (c) $MoSe_2$-NiSe-C, and (d) $MoSe_2$-NiSe-$NiSe_2$.

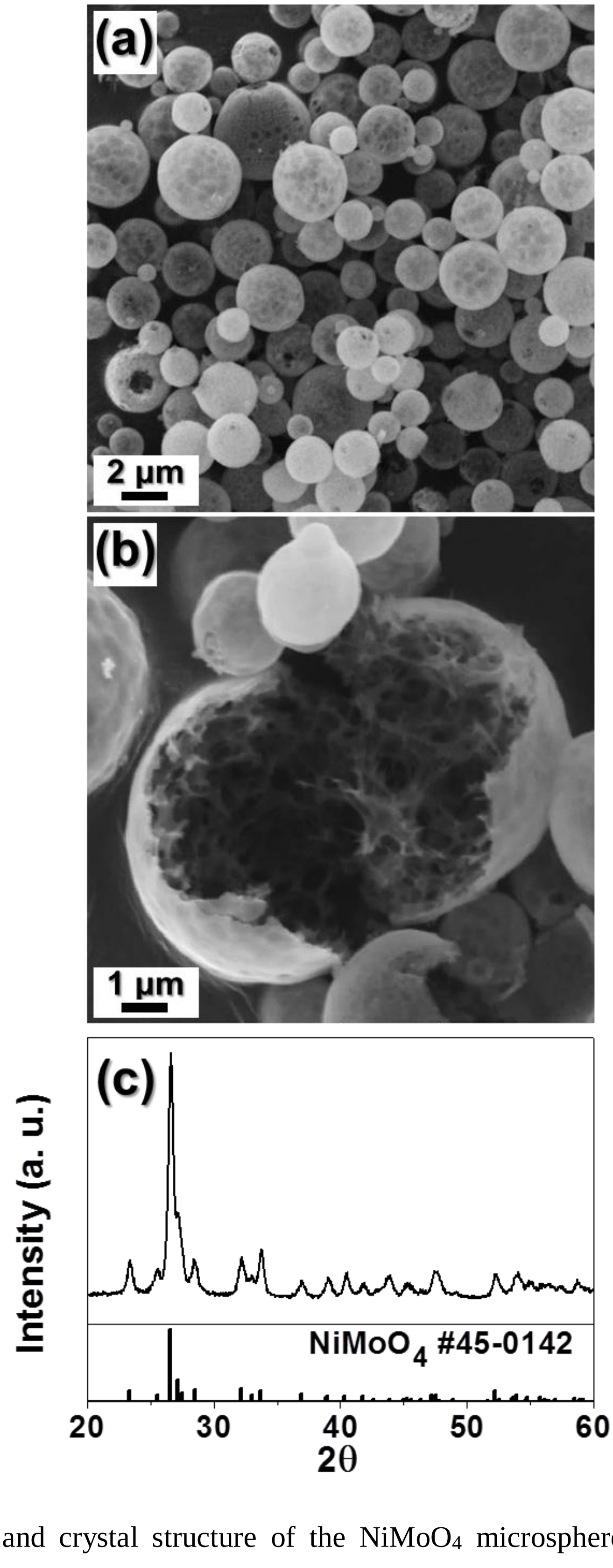

Fig. S3. Morphology and crystal structure of the $NiMoO_4$ microspheres with empty nanovoids obtained from oxidation of the spray dried powders at 500 ^oC: (a) low resolution and (b) high resolution SEM images, and (c) XRD pattern.

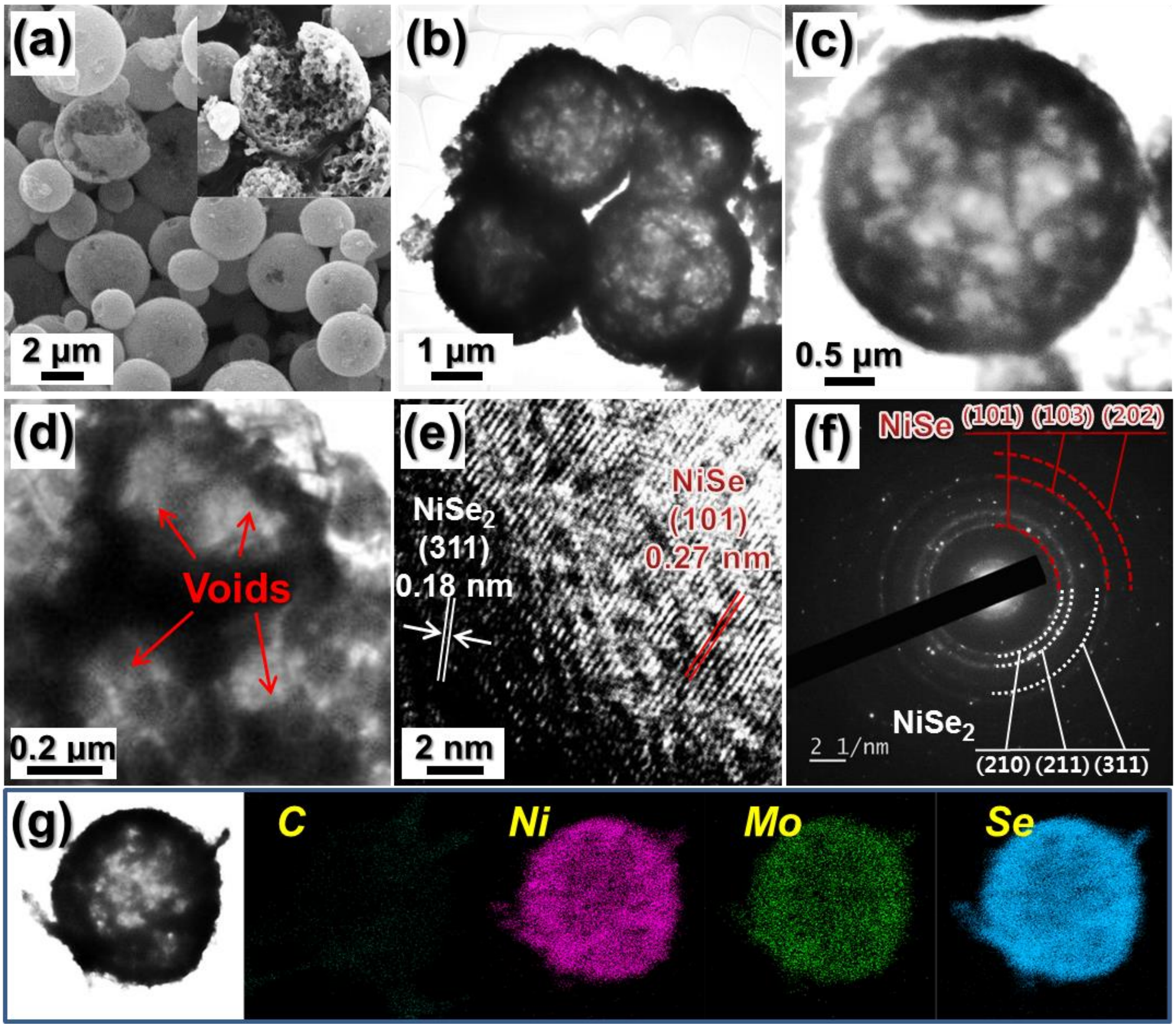

Fig. S4. Morphologies, SAED pattern, and elemental mapping images of the multiroom-structured $MoSe_2$-NiSe-$NiSe_2$ microspheres: (a) SEM image, (b-d) TEM images, (e) HR-TEM image, (f) SAED pattern, and (g) elemental mapping images.

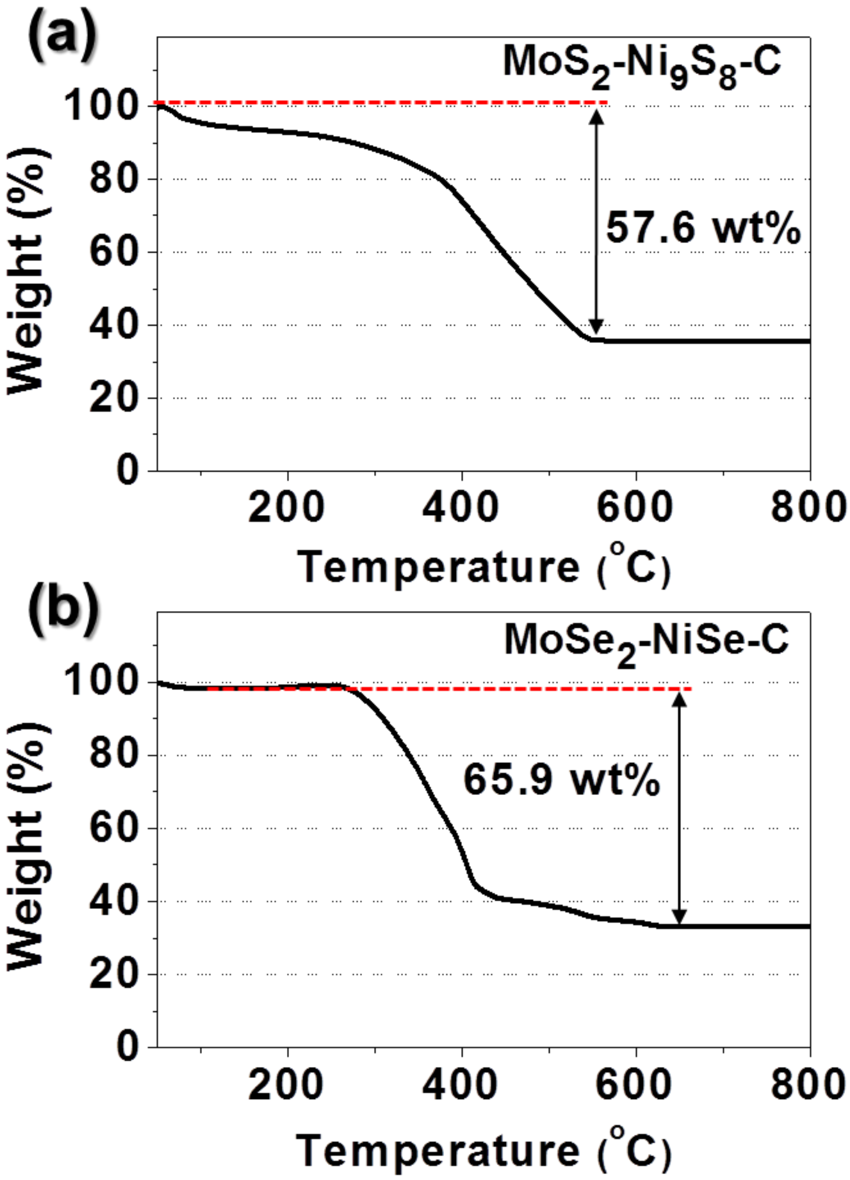

Fig. S5. TG curves of the multiroom-structured (a) MoS_2-Ni_9S_8-C and (b) $MoSe_2$-NiSe-C microspheres.

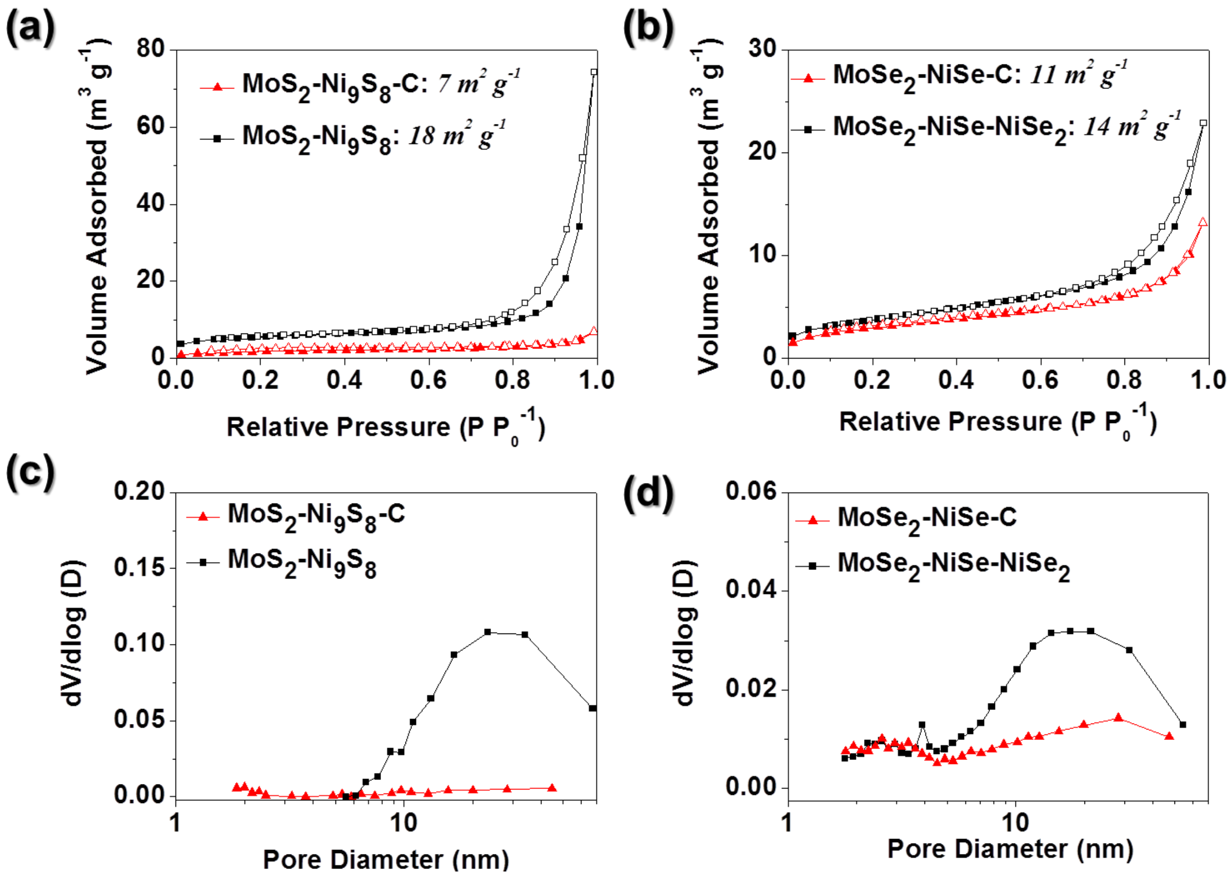

Fig. S6. (a, b) N_2 adsorption and desorption isotherms and (c, d) BJH pore size distributions of the multiroom-structured MoX_2-NiX_y (X= S or Se) and MoX_2-NiX_y-C.

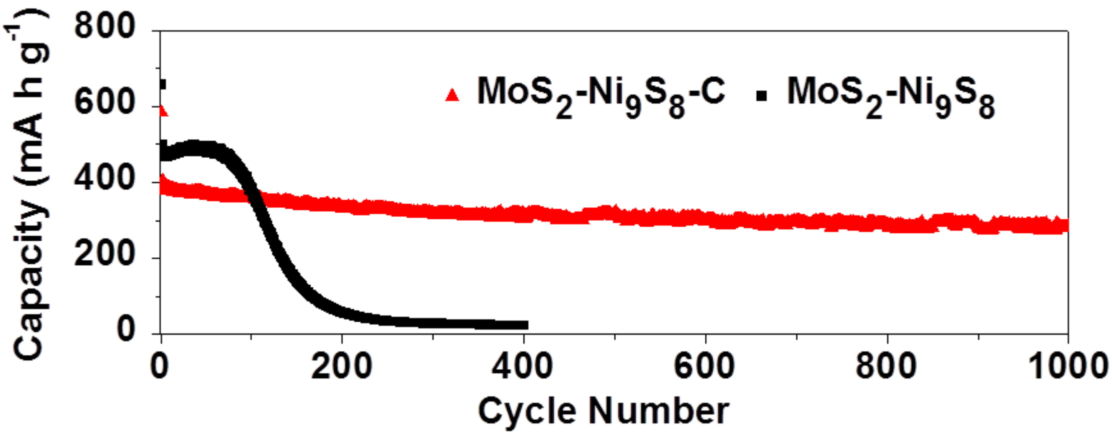

Fig. S7. Long-term cycling performances of the multiroom-structured MoS_2-Ni_9S_8-C and MoS_2-Ni_9S_8 microspheres at a current density of 0.5 A g^{-1}.

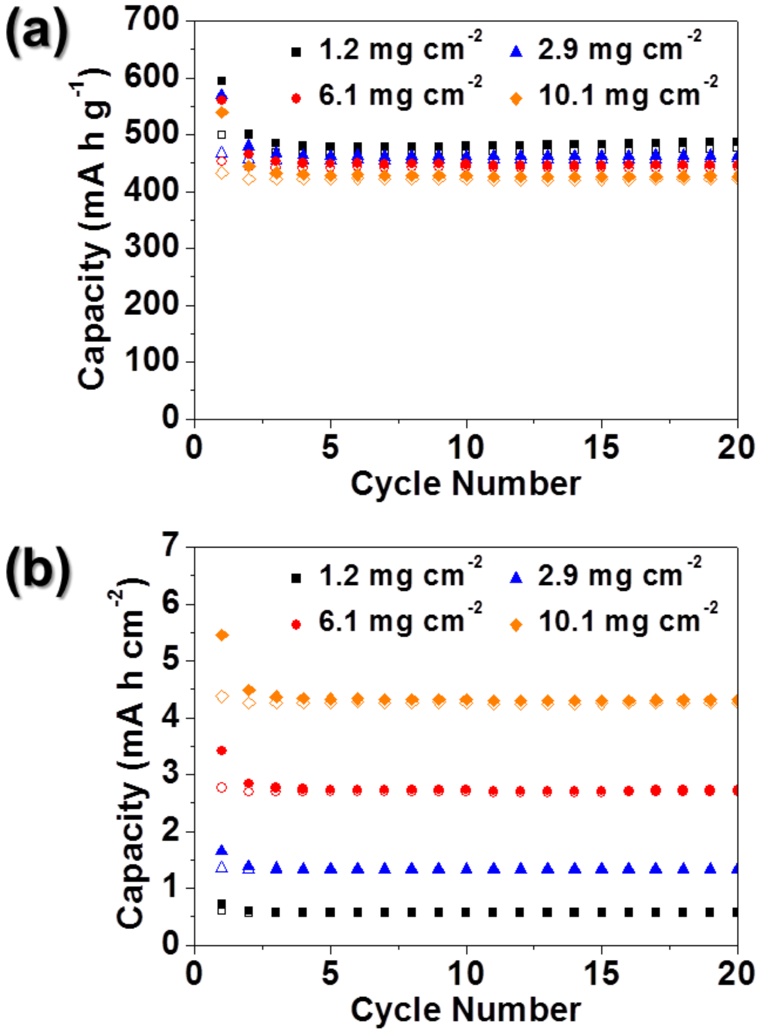

Fig. S8. (a) Gravimetric and (b) areal capacities of the MoS_2-Ni_9S_8 microspheres at different active material mass loadings on the electrode.

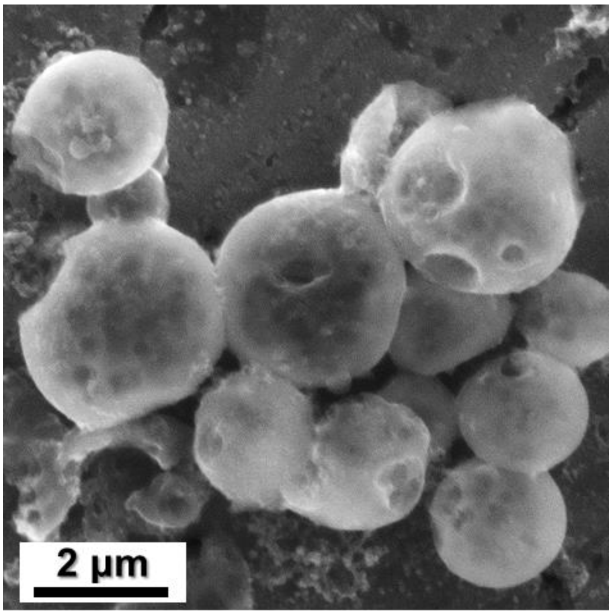

Fig. S9. Morphology of the multiroom-structured MoS_2-Ni_9S_8-C microspheres after 1000 cycles.

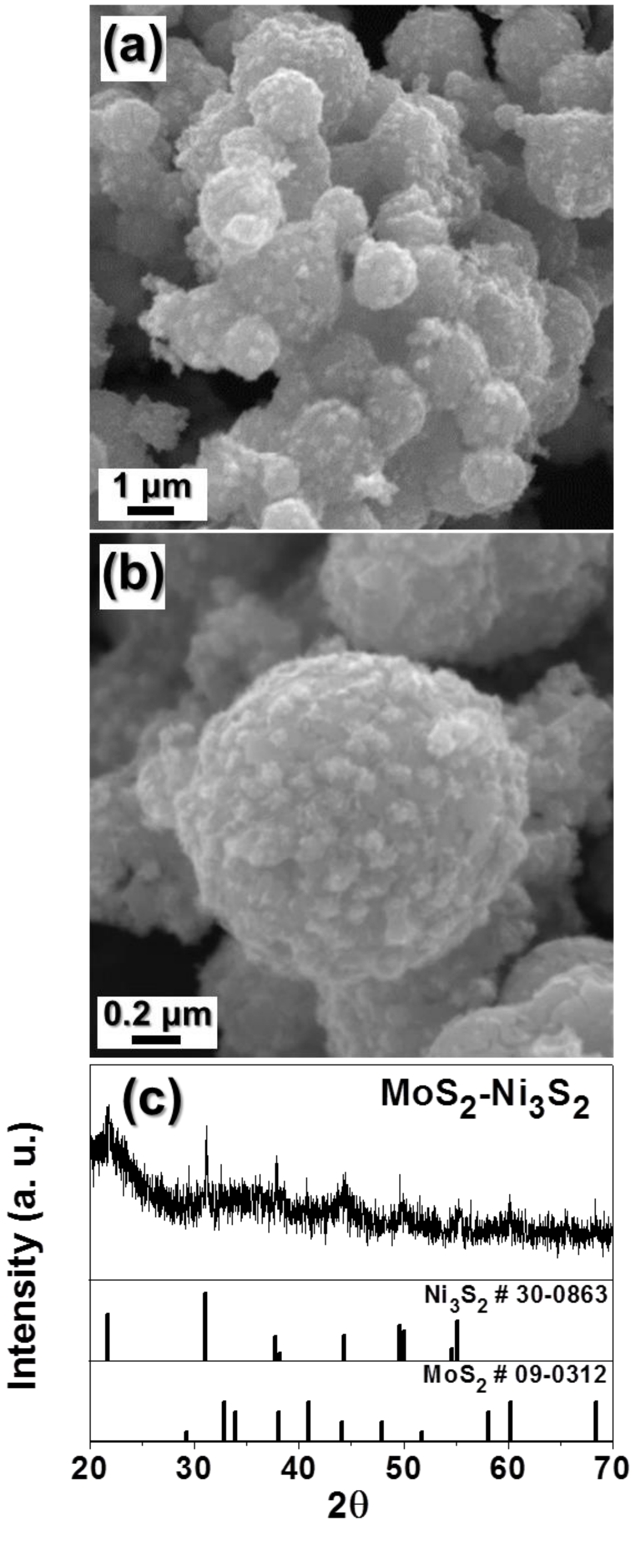

Fig. S10. (a, b) Morphologies of the MoS_2-Ni_3S_2 powders powders obtained by sulfidation of the microspheres prepared from the spray solution without dextrin: (a) low resolution and (b) high resolution SEM images, and (c) XRD pattern.

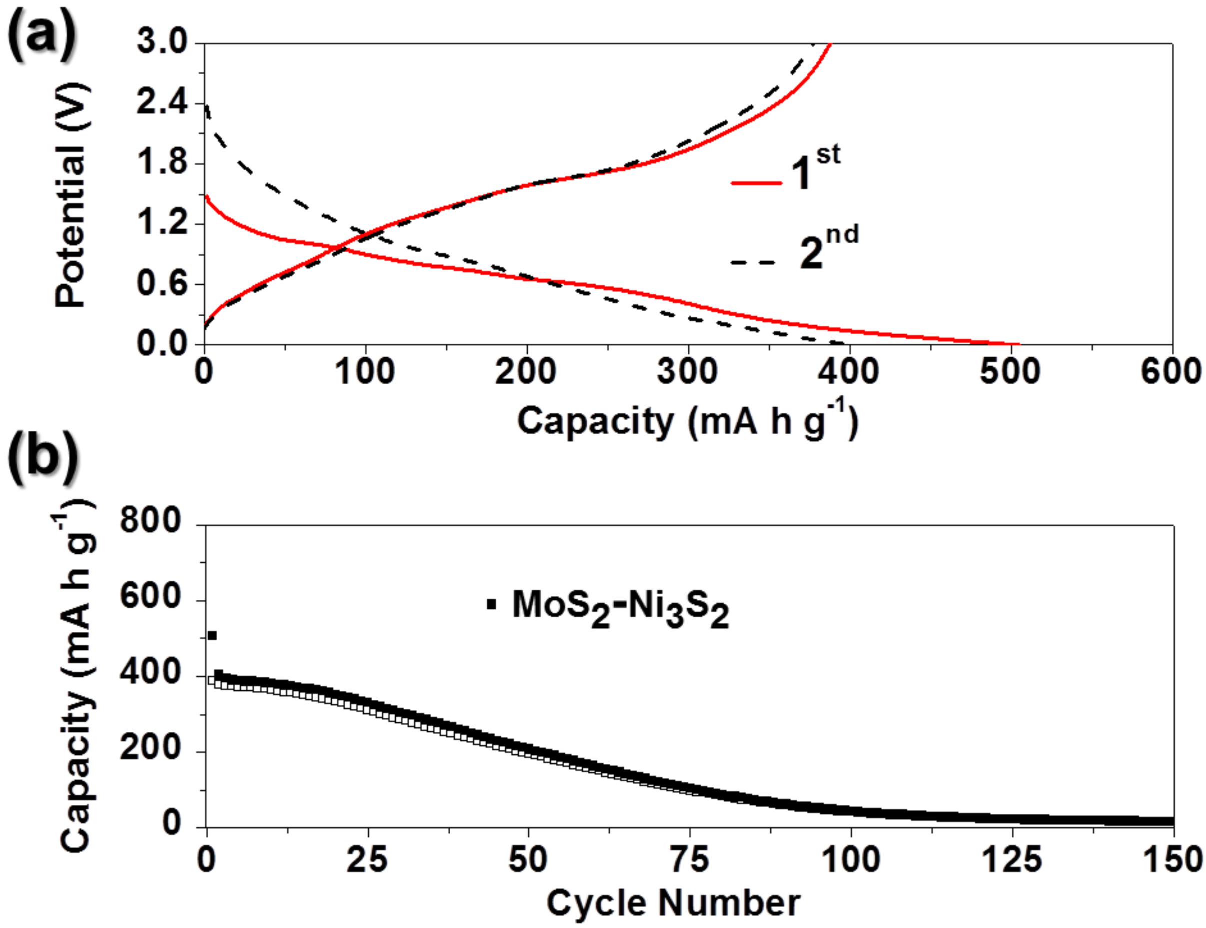

Fig. S11. Electrochemical properties of the MoS_2-Ni_3S_2 powders obtained from the microspheres prepared from the spray solution without dextrin: (a) first and second charge-discharge curves at a current density of 0.5 A g^{-1} and (b) cycling performance at a current density of 0.5 A g^{-1}.

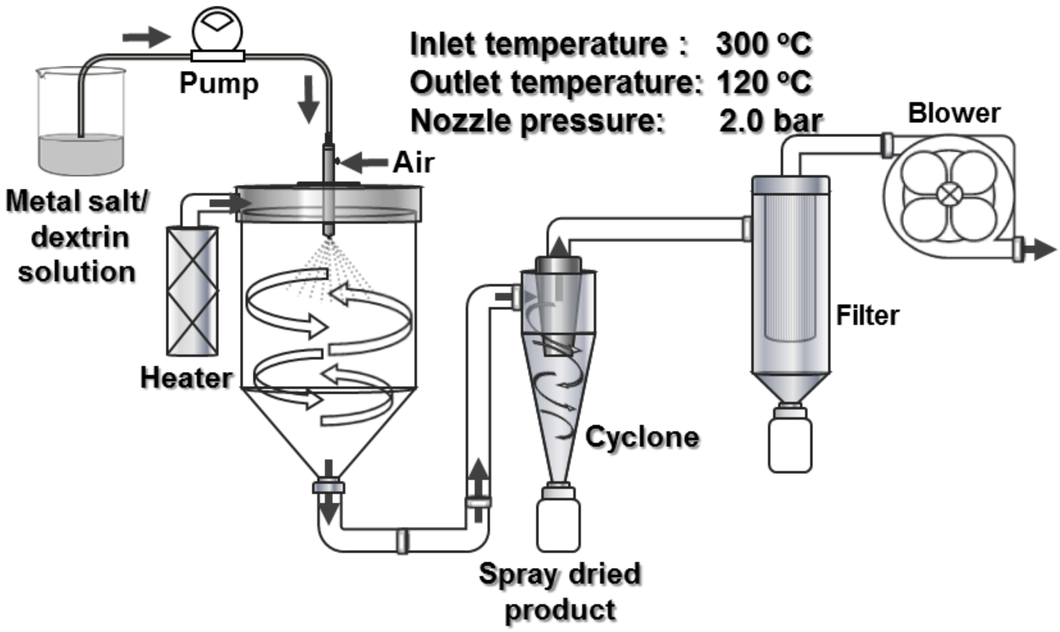

Fig. S12. Schematic diagram of the pilot-scale spray drying system.

Table S1. Electrochemical properties of various nanostructured NiS_x and MoS_x materials applied as sodium-ion batteries reported in the previous literatures.

Electrode materials	Preparation method	Current density [$A\ g^{-1}$]	Initial discharge/charge capcities [$mA\ h\ g^{-1}$]	Discharge capacity [$mA\ h\ g^{-1}$] and (cycle number)	Rate capacity [$mA\ h\ g^{-1}$]	Ref.
Layered nickel sulfide-reduced graphene oxide composites	Microwave-assisted method	0.1	665/513	392 (50)	346 (1.0 $A\ g^{-1}$)	[36]
NiS_x/CNT@C	Solvothermal	0.1	760/450	340 (200)	208 (2.0 $A\ g^{-1}$)	[35]
Nickel disulfide–graphene nanosheets	Hydrothermal	0.087	833/518	313 (200)	168 (1.6 $A\ g^{-1}$)	[S1]
Porous clustered network-like Ni_3S_2/Ni	Hydrothermal	0.05	373/320	315 (100)	218 (0.8 $A\ g^{-1}$)	[S2]
MoS_2/electrospun carbon nanofiber composite	Electrospinning	1.0	754/483 at 0.05 $A\ g^{-1}$	198 (500)	148 (3.2 $A\ g^{-1}$)	[S3]
Nitrogen-Doped Carbon Embedded MoS_2 Microspheres	Hydrothermal	0.15	810/579	340 (150)	180 (3.0 $A\ g^{-1}$)	[28]
MoS_2 nanosheets decorated Ni_3S_2@MoS_2 coaxial nanofibers	Hydrothermal	0.2	707/593 at 0.1 $A\ g^{-1}$	483 (100)	356 (3.0 $A\ g^{-1}$)	[27]
MoS_2-Ni_9S_8 composite microspheres	Spray drying	0.5	657/499	459 (80)	428 (3.0 $A\ g^{-1}$)	***This work***
MoS_2-Ni_9S_8-C composite microspheres	Spray drying	0.5	584/380	285(1000)	307 (3.0 $A\ g^{-1}$)	***This work***

Table S2. Electrochemical properties of various nanostructured $NiSe_x$ and $MoSe_x$ materials applied as sodium-ion batteries reported in the previous literatures.

Electrode materials	Preparation method	Current density [$A\ g^{-1}$]	Initial discharge/charge capcity [$mA\ h\ g^{-1}$]	Discharge capacity [$mA\ h\ g^{-1}$] and (cycle number)	Rate capacity [$mA\ h\ g^{-1}$]	Ref.
$NiSe_2$-rGO-C composite nanofibers	Electrospinning	0.2	717/516	468 (100)	243 (3.0 $A\ g^{-1}$)	[38]
core-shell NiSe/C nanospheres	Hydrothermal	0.1	493/398	283 (50)	172 (0.5 $A\ g^{-1}$)	[S4]
Fullerene-like $MoSe_2$ nanoparticles-embedded CNT balls	Spray pyrolysis	0.2	626/457	296 (250)	280 (3.0 $A\ g^{-1}$)	[13]
C-$MoSe_2$/ reduced graphene oxide composite	Hydrothermal	0.2	774/483	445 (350)	284 (2.0 $A\ g^{-1}$)	[29]
$MoSe_2$ microspheres	Colloidal	0.042	520/430	345 (200)	298 (0.4 $A\ g^{-1}$)	[S5]
$MoSe_2$ nanosheets grown on carbon cloth	Solvothermal	0.2	888/~453	387 (100)	240 (2.0 $A\ g^{-1}$)	[30]
$MoSe_2$-NiSe-$NiSe_2$ composite microspheres	Spray drying	0.5	608/450	291 (80)	-	***This work***
$MoSe_2$-NiSe-C composite microspheres	Spray drying	0.5	546/382	386 (80)	301 (3.0 $A\ g^{-1}$)	***This work***

[S1] T. Wang, P. Hu, C. Zhang, H. Du, Z, Zhang, X. Wang, S. Chen, J. Xiong, G. Cui, *ACS Appl. Mater. Interfaces*, 2016, **8**, 7811-7817.

[S2] X. Song, X. Li, Z. Bai, B. Yan, D. Li, X. Sun, *Nano Energy*, 2016, **26**, 533-540.

[S3] C. Chen, G. Li, Y. Lu, J. Zhu, M. Jiang, Y. Hu, L. Cao, X. Zhang, *Electrochim. Acta*, 2016, 222, 1751-1760.

[S4] Z. Zhang, X. Shi, X. Yang, *Electrochim. Acta*, 2016, **208**, 238-243.

[S5] H. Wang, L. Wang, X. Wang, J. Quan, L. Mi, L. Yuan, G. Li, B. Zhang, H. Zhong, Y. Jiang, *J. Electrochem. Soc.*, 2016, **163**, A1627-A1632.